Bimetallic Thermal Resists Potential for Double Exposure Immersion Lithography and Grayscale Photomasks

James M. Dykes, Calin Plesa, Chinheng Choo, and Glenn H. Chapman*
School of Engineering Science, Simon Fraser University, Burnaby, BC V5A 1S6, Canada

ABSTRACT

Double exposure/patterning is considered the best candidate for extending 195nm optical lithography below 40nm resolution. However, double exposure techniques require a resist where the exposures do not add linearly to produce the final result. A class of negative thermal resists that show this effect are bimetallic thin-films consisting of Bi/In or Sn/In. The films are bi-layered structured until sufficiently heated by a laser exposure pulse (7 mJ/sq. cm for 4 nsec). Experiments with interference lithography at 266nm in air demonstrated that Bi/In resists have a resolution limit <42nm, the exposure system limit. As a first investigation into the resist's potential for immersion lithography, the response of bimetallic resists to immersion lithography was examined. The Sn/In film used demonstrated successful development as thermal resist for immersion exposures and the power level required to convert the film was only slightly higher than the level required for exposing the film in air.

Bimetallic films have demonstrated transmittances <0.1% when unexposed and >60% when highly exposed to an Argon laser, enabling their application as grayscale photomasks. However, direct laser-writing of the photomasks causes fine variations in their transparency due to the laser beam's Gaussian power profile. To correct this problem, a beam-shaping mask was designed to manipulate the power profile of the laser. To help measure mask transparency at a resolution suitable for characterizing a photomask, two photodiode sensors were added to the writing system. The profiling ability offered by the modified system allows the use of test structures 100x smaller then previously required.

Key words: Bimetallic Thin-Film, Grayscale, Photomask, Thermal Resist, Direct-write, Interference Lithography, Immersion Lithography, Transparency

1. INTRODUCTION

Optical lithography is facing a significant challenge due to delays in the movement to new, shorter, wavelengths. The 157 nm wavelength was killed by the development of immersion lithography at 193 nm. The EUV 13.4 nm sources are currently delayed for several years. At the same time exposure systems have reached a point where little improvement can be expected in NA (Numerical Aperture) and k_1. Without new optical materials, NA saturates at the current levels while k_1 is near its theoretical limit. These results suggest a current resolution limit of 35 nm if the wavelength is not reduced. To further reduce the resolution limit, many authors propose using double exposure/double patterning techniques. Double exposure employs two phase shift masks, each with half of the pattern (that is patterns spaced 2x the desired pitch, refer to Figure 1)[1]. The resist is exposed by the first mask then by the second prior to development. With the second exposure using a mask that is shifted by half the resolution limit, the two-exposures combine to achieve a pattern with a pitch 50% smaller than possible with a single exposure.

However, the inherent requirement for double exposure techniques to work is the need for a resist that breaks the superposition principal. In other words, the resulting exposure cannot respond as a linear sum of the two separate exposures but rather needs to be a non-linear addition

$$f(\mathrm{Exp}_1) + f(\mathrm{Exp}_2) \neq f(\mathrm{Exp}_1 + \mathrm{Exp}_2). \quad (1)$$

By breaking the superposition principal, the resist would also not exhibit reciprocity, which allows resists to accumulate an exposure by repeated pulses. Reciprocity is required for resists patterned using current Excimer laser exposure systems where a single laser pulse is kept below the resist's threshold and the full exposure is the repeated application of these sub-threshold pulses. Existing organic resists follow both superposition and reciprocity which

* glennc@cs.sfu.ca; phone 1-604-291-3814; fax 1-604-291-4951; http://www.ensc.sfu.ca/people/faculty/chapman/; School of Engineering Science, Simon Fraser University, 8888 University Drive, Burnaby, BC V5A 1S6, Canada

means they are not suited for double patterning. However, thermal resists operate by a different principal in which the optical exposure induces a temperature change that causes the resist's reaction when the temperature exceeds a given threshold. Thus, sub-threshold exposures are not accumulated (because the heat flows away between pulses) allowing thermal resists to break both superposition and reciprocity in the manner needed for double exposure techniques.

We have been investigating bimetallic films as thermal resists for several years[2] and they have demonstrated many of the characteristics required for double exposure techniques. They are formed by depositing two thin layers (typically 15 nm) of metals, typically Bismuth on Indium (Bi/In) or Tin on Indium (Sn/In), onto a given substrate which is then exposed with the short duration (4-10 nsec.) laser pulses of an Excimer system. The exposure (at 7 mJ/cm^2 or organic resist sensitivity) heats the film and once elevated above a certain threshold causes it to convert into a transparent eutectic oxide, similar to ITO. The converted material can then be developed using a diluted RCA-2 solution. The entire process of patterning and developing a bimetallic film as a thermal resist is shown in Figure 2.

This paper examines the characteristics of bimetallic resists with respect to what needs to be investigated for their application towards double exposure techniques; in particular, what are the resolution limits of this resist. In addition, the double exposure systems being developed will also utilize immersion conditions in which the resist is exposed when immersed in a liquid with a high index of refraction. Thus, we will not only discuss the resolution limits of bimetallic thin-films but also their application towards immersion lithography. As a first step in determining bimetallic film's potential as a resist for double exposure immersion lithography, lines are patterned in both air and water-immersed conditions. Utilizing profilometry and microscopic images, the resist is examined prior to and after development for successful resist creation under different exposure powers.

In addition to their application as thermal resists, bimetallic films have another unique quality. The BiIn oxide formed is transparent at 365 nm and longer wavelengths. Furthermore, the level of transparency is a direct function of the laser power used for the exposure, ranging in transparency from <0.1% when unexposed to >60% when highly exposed. The wide range in transparency enables them to be used for direct-write grayscale photomasks. Grayscale photomasks are typical used in the production of smoothly varying 3D structures such as those required for microlenses, diffractive optics, and MEMS. Illustrated in Figure 3 is the production of a direct-write bimetallic film grayscale.

In developing bimetallic films for use as a grayscale photomasks, previous experiments consisted of writing mask patterns using a beam-shaped laser[3]. The beam-shaping's purpose was to transform the beam from its non-uniform Gaussian power profile into a more uniform "top-hat" beam and reduce transparency variations in the written mask. For this paper, previously written masks are examined further for improvements by scanning them using the mask-writing system modified into an OD/transparency profiler.

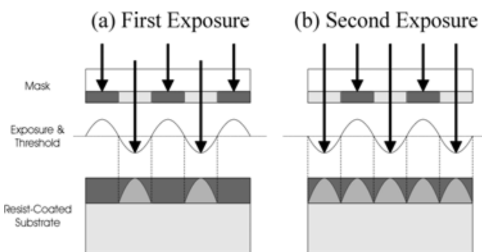

Figure 1: Theory of operation for a double exposure system: (a) first exposure and (b) second exposure with half pitch shift in the mask. The resulting exposure has twice the resolution of the individual exposures.

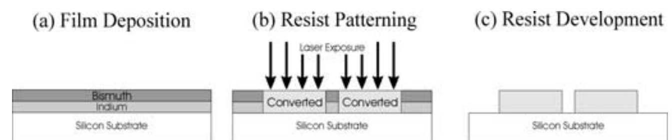

Figure 2: Bimetallic thin-films used as thermal resists: (a) film sputter deposition, (b) patterning of the resist by laser exposure, and (c) resulting resist structure after development.

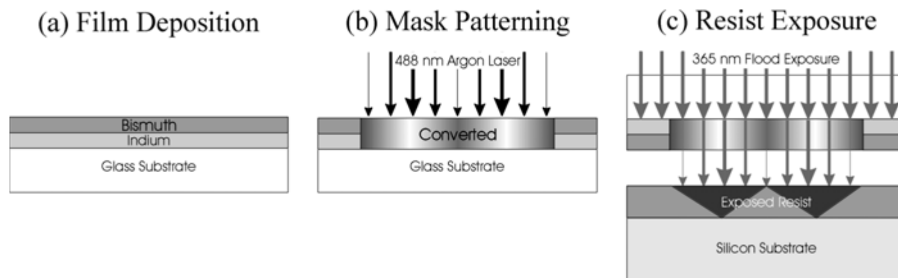

Figure 3: Bimetallic thin-films used as grayscale photomasks: (a) film sputter deposition, (b) grayscale mask patterning by direct-write laser exposure (488 nm Argon Laser), and (c) resist exposure through the mask (365 nm flood exposure).

2. BIMETALLIC FILM DEPOSITION PATTERNING

Unlike organic resists each layer of the bimetallic film is DC or RF sputtered onto the desired substrate. For our experiments, glass microscope slides were used as the underlying substrate and the sputtering was performed using a Corona Vacuum Coater DC/RF Magnetron sputter. The bimetallic films can consist of a variety of different metals; however, typical combinations for the production of photomasks are Bi/In and Sn/In. The sputter targets used are 2" in diameter and are 99.99% pure. The sputtering rates for the three materials are shown in Table 1.

The deposition process starts by pumping the vacuum chamber down to a base pressure of 6 x 10^{-3} mTorr. During deposition, Argon gas is introduced into the sputtering chamber at 10 sccm and the chamber is maintained at 4 mTorr pressure. The film layers are then deposited without an air break.

With the film deposited, the next step is to expose and pattern the film. Two setups have been used for this purpose, one designed to test the resolution limits of the bimetallic film and is based on an Nd:YAG pulsed laser, the other uses an Argon CW laser, which is more readily available and is sufficient for our initial experimentation into immersion lithography for bimetallic films.

Table 1: Sputtering Rates for Bi, In, and Sn

Metal	Argon Pressure (mTorr)	DC bias (V)	Current (A)	Watt·Min	Deposit rate (Å/W·min)
Bi	4	470	0.23	2500	12
In	3	450	0.23	2500	4
Sn	3	432	0.23	2500	6

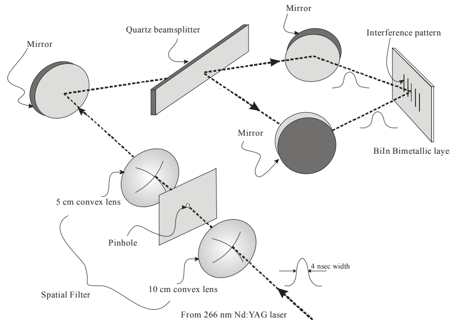

Figure 4: Experimental setup to create interference pattern using 4th harmonic of Nd:YAG laser (266 nm).

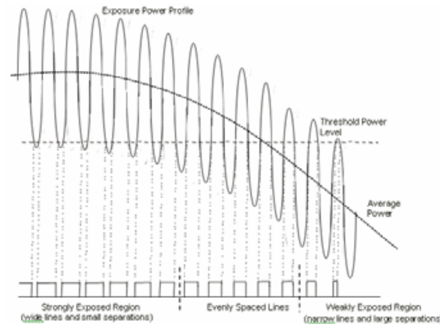

Figure 5: Interference lithography exposure. The widths of the lines and spaces are dependent upon the exposure threshold of the film and average power of the exposure.

3. BIMETALLIC FILM INTERFERENCE PATTERNING: RESOLUTION LIMIT

One of the most important investigations regarding bimetallic thin-film resists is to determine what their resolution limit is. However, an important implication regarding the lack of reciprocity for these double exposure resists is that the exposure energy must be delivered in a single pulse of a <10 nsec. This result means that even though the BiIn resist has organic level sensitivity, many existing interference lithography tools cannot be used directly to determine its resolution limits as they use multiple exposures. Consequently, to test the resolution limit for our bimetallic thin-film resists, we created an interference lithography system using an Nd:YAG laser with a 4th harmonic crystal producing 266 nm pulses of 4 nsec in duration[4]. Passed through a spatial filter and 50/50 beam-splitter, the beams are then diverted back towards the film where they interfere and expose it, as shown in Figure 4 and Figure 5. In estimating the resolution limit for bimetallic films, a Bi/In film deposited on Silicon was patterned with the Nd:YAG laser operating at its highest setting of 89 mJ per pulse at 266 nm per 4 ns pulse over an area ~ 1cm^2. Since the pitch or period of the parallel line interference pattern is equal to $\lambda/(2\sin\theta)$, where λ is the laser wavelength and θ is the incident angle, finer line patterns can be produced by increasing the incident angle. However, increasing the angle also decreases the laser energy density on the film; thus, the largest incident angle possible becomes a function of the laser's highest power. The incident angle for our setup was set to about 18°. Any further increases to the incident angle would inhibit the production of the interference pattern due to the decreased exposure of the film. Once patterned, the Bi/In film was then developed using a diluted RCA-2 solution of $HCl:H_2O_2:H_2O$ at a concentration ratio of 1:1:73. Typically a 1:1:48 ratio is used for the development of Bi/In films[5]; however, due to the weaker exposure of the film, a weaker concentration was chosen to prevent the developer from removing less exposed regions. Figure 6 illustrates SEM images of the developed patterns; a conductive

layer of 6 nm to 8 nm Au was DC-sputtered onto the bimetallic films for better SEM imaging. Figure 6 (a) shows a region with well-defined line-gaps that are 68 ± 12 nm wide, while Figure 6 (b) shows a region of the sample that was weakly exposed where the lines are thin and the separations are far apart. The narrowest line width seen in this region is 83 ± 10 nm; however, the lines in this area appear to have a distinct straight-edge on one side and a relatively uneven edge on the other. The uneven edge may be due to the interference pattern smearing out on the weaker exposed ends. Lastly, Figure 6 (c) shows the smallest line-gap obtained from our experiments: estimated to be 42 ± 5 nm. We feel this is not the absolute resolution limit of the films but is rather the limit of our lithography system, which is working at a longer 266 nm wavelength in air rather than the 193 nm wavelength used in immersion lithography.

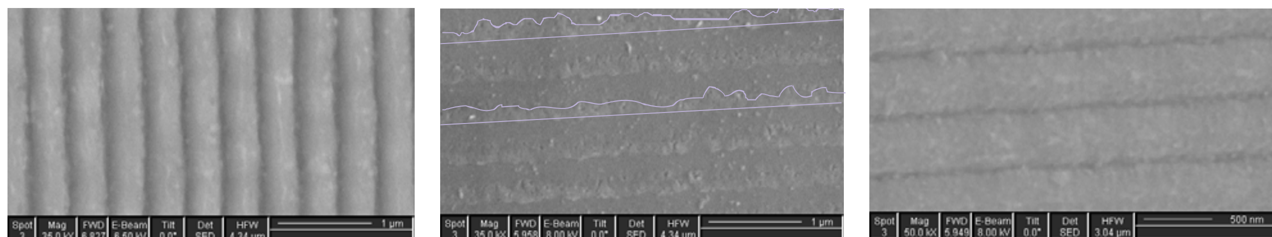

Figure 6: SEM images for developed interference patterns: (a) pattern in strongly exposed region showing wide lines, (b) pattern in weakly exposed region showing wide spaces, and (c) pattern showing deep submicron spaces.

4. BIMETALLIC FILM DIRECT-WRITE PATTERNING: IMMERSION TESTING

While the exposure of bimetallic resists must occur in a single pulse, the duration of the exposure can range from nsec to millisec. For patterning both our immersion lithography and grayscale photomask creation experiments, we used a raster-scanning technique involving a Coherent Argon 488nm/514nm CW laser whose power is modulated by a Conoptics electro-optical crystal shutter. After modulation, the beam is guided onto the stage of an Anorad X-Y-Z table and focused by either convex or objective lenses onto the film. This setup gives wide control over both the patterns being created and the exposure power. To produce grayscale masks, the X-Y-Z table moves in a raster-scan manner writing the photomask one line at a time from a 256 gray-level bitmap. As the laser moves to write a line, a function generator loaded with the desired pattern controls the electro-optical shutter and modulates the power of the laser beam. Figure 7 illustrates the mask-writing system used at Simon Fraser University.

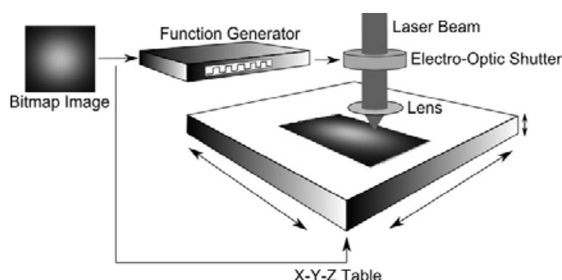

Figure 7: Mask-writing system used in the production of grayscale photomasks on bimetallic films.

5. IMMERSION EXPOSURE OF BIMETALLIC FILMS

For bimetallic films to be useful for double exposure techniques the effects of immersion lithography, (or underwater laser exposure) on the resist had to be investigated. The bimetallic films themselves, unlike organic resists, are not affected by water either before or after exposure[2], so the question is what happens during the exposure. For these tests an 80 nm thick Sn/In bimetallic film on a glass substrate was patterned with lines of varying laser exposure power in both air and water-immersed conditions. Sn/In resists were used because they are less sensitive than Bi/In and hence immersion effects would be more noticeable. We varied the laser power and exposure time (velocity of the X-Y table) under both air and water-immersed conditions; furthermore, we used both large (10 μm) and small (2 μm) laser spots so we could observe the process as it occurred. Figure 8 shows microscope images of the exposed bimetallic films for various exposures below 300mW and writing speeds up to 10000 μm/s (i.e. 1 millisec exposures). There are 4 lines spaced 50 μm apart for each exposure power. Examining the air-written results for the 50 mm convex lens (10 μm spot), shown in Figure 8 (a) and (c), the width of the lines vary significantly with the laser power Ranging between 6.7 μm to

42.0 μm wide as shown in Table 2, the variations represent the thermal flow/thresholds location for these long exposures. Furthermore, as the velocity increased, the lines appear to be less oxidized since the energy that the film was exposed with was also reduced. Using the 50x objective lens (2 μm spot), shown in Figure 8 (b) and (d), the lines are focused down to between 1.8 μm to 7.0 μm wide and visually look less affected by changes in the velocity. The lack of changes with velocity for the 2 μm spot-size is likely due to the writing beam's increased power density at the exposure site.

Figure 9 shows microscope images of the water-immersed films exposed with various laser exposure powers below 300 mW and at writing speeds up to 10000 μm/s. There are 4 repeated lines spaced 50 μm apart for each exposure power. Examining the immersed results for the 10 μm spot-size, shown in Figure 9 (a), (c) and (e), the widths of the lines vary significantly with the laser power, ranging between 8.0 μm to 39.3 μm wide as shown in Table 3. Increasing the velocity also affected the immersed results more, as shown in Figure 9 (e) and (f), where the increased velocity significantly reduced the effective width of the lines.

Comparing the immersion and air results, several points are notable. First, it is clear that the bimetallic resists can operate under immersion conditions. While Table 2 and Table 3 show that the lowest powers are not exposed under immersion conditions, all the other powers are. Given the reflective losses that occur at the air/water interface (at least 5%); the slightly increased power required is modest and suggests that heat flow to the water is not a limiting factor at short exposure times. Secondly, it is noted that at the highest powers/slowest speed the smallest spot size may still generate large lines. This result is because the area heated above the threshold becomes large under these conditions.

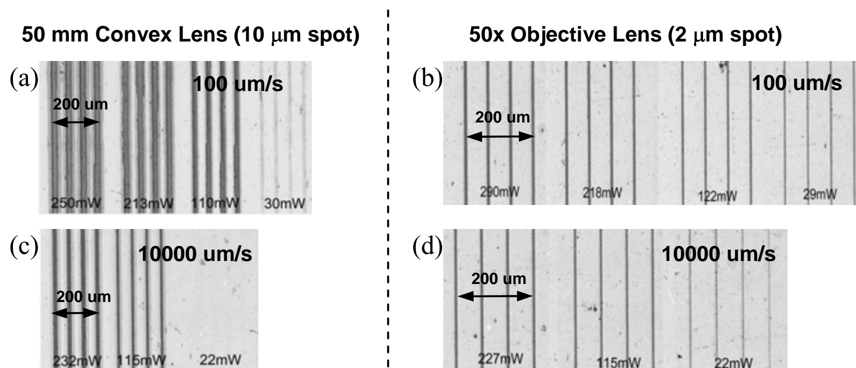

Figure 8: Front-lit, 80 nm thick Sn/In bimetallic film exposed in air with various laser exposure powers below 300mW: (a) written using 100 μm/s and a 10 μm spot, (b) 100 μm/s and a 2 μm spot, (c) 10000 μm/s and a 10 μm spot, and (e) 10000 μm/s and a 2 μm spot.

Table 2: Line Widths for Air-Written Lines

Writing Velocity (μm/s)	50 mm Convex Lens (10 μm spot)		50x Objective (2 μm spot)	
	Exposure Power (mW)	Line Widths (μm)	Exposure Power (mW)	Line Widths (μm)
100	30	11.4 – 13.4	29	2.3 – 2.9
100	110	20.8 – 22.1	122	3.0 – 4.1
100	213	31.9 – 36.8	218	3.9 – 5.2
100	250	36.8 – 42.0	290	5.6 – 7.0
1000	29	6.7 – 10.1	28	1.8 – 3.0
1000	116	20.9 – 22.9	117	3.9 – 5.1
1000	212	31.7 – 35.1	232	5.4 – 6.8
10000	22	0	22	2.9 – 3.4
10000	115	21.5 – 25.5	115	2.9 – 3.5
10000	232	29.5 – 30.9	227	3.6 – 4.7

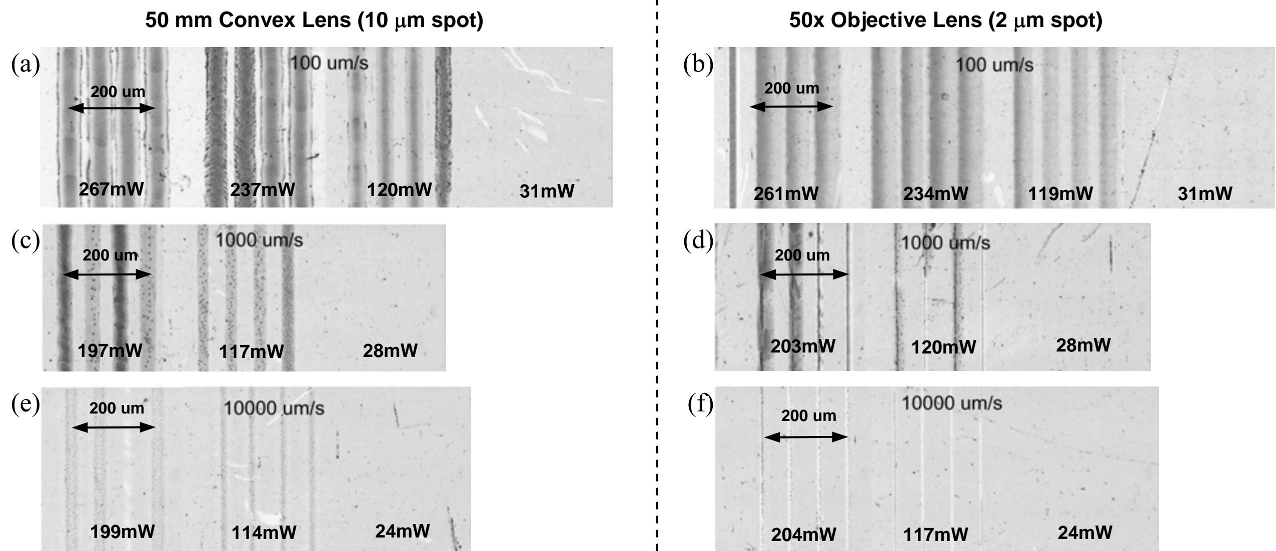

Figure 9: Front-lit 80 nm thick Sn/In bimetallic thin-film exposed in water-immersed conditions with various laser exposure powers, writing velocities and laser spot sizes: (a) written using 100 μm/s and the laser beam focused to a 10 μm spot, (b) 100 μm/s and a 2 μm spot, (c) 1000 μm/s and a 10 μm spot, (d) 1000 μm/s and a 2 μm spot, (e) 10000 μm/s and a 10 μm spot, and (f) 10000 μm/s and a 2 μm spot.

Table 3: Line Widths for Lines Written in Water-Immersed Conditions

Writing Velocity (μm/s)	50 mm Convex Lens (10 μm spot)		50x Objective (2 μm spot)	
	Exposure Power (mW)	Line Widths (μm)	Exposure Power (mW)	Line Widths (μm)
100	31	0	31	0
100	120	26.7 – 29.6	119	27.4 – 32.1
100	237	35.0 – 37.0	234	35.3 – 45.6
100	267	38.4 – 39.3	261	40.1 – 43.4
1000	28	0	28	0
1000	117	17.2 – 20.5	120	2.0 – 3.0
1000	197	26.1 – 27.5	203	2.8 – 27.8
10000	24	0	24	0
10000	114	8.0 – 8.8	117	1.7 – 4.1
10000	199	17.7 – 18.3	204	1.9 – 3.4

The significant variations in the line widths under the water-immersed conditions are best illustrated in Figure 9 (d). These variations are the result of an air or steam bubble forming at the exposed site on the film, altering the laser beam's behavior through the water. When present, the bubble causes the lines to become 2x to 10x times larger. Furthermore, the bubble follows the laser beam as it patterns the bimetallic film and is more consistent in the slower 100 μm/s scans compared to the faster scans, as shown in Figure 10. Examining the profiles of the exposed lines prior to development, Figure 11 shows some example profiles for the lines written when immersed in water.

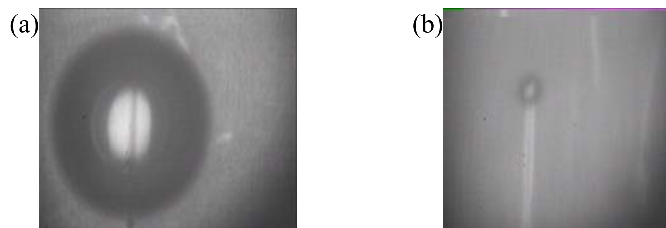

Figure 10: Steam bubble formed during the laser writing process for water-immersed Sn/In bimetallic film. The lines being written are with a 62 mW beam and at a velocity of (a) 100 μm/s and (b) 1000 μm/s.

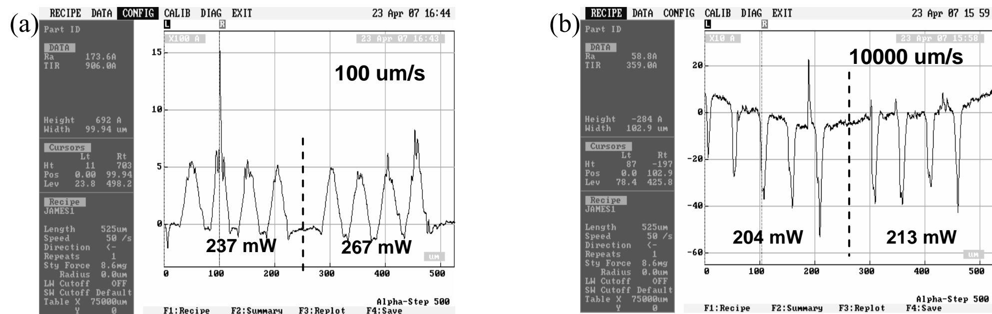

Figure 11: Surface profiles for the 80 nm thick Sn/In bimetallic film exposed in water-immersed conditions: (a) lines written at 100 μm/s and a 10 μm spot, and (b) written at 10000 μm/s and a 2 μm spot.

Profiles indicate that when exposed with the bubble the film oxidizes and appears as a height increase in the profile, which is the same as the profiles taken for the air exposed results. Conversely, at high power densities there is a height decrease in the profile when the film is immersed, indicating removal of the resist. A possible explanation is that under the high power and rapid scanning conditions rather than creating a uniform steam layer over the film's surface, many small steam bubbles are quickly created and collapse. These collapsing bubbles cause a well known cavitation effect where the acoustic shock waves from their collapse tear apart the adjacent layer. While this issue is being investigated, it should not occur in a standard stationary exposure condition.

6. DEVELOPMENT OF EXPOSURED BIMETALLIC FILMS AS THERMAL RESIST

Having exposed the bimetallic film underwater, the next stage was to develop the bimetallic film for use as a thermal resist. Developing the film as a thermal resist was done using a diluted RCA-2 solution of $HCl:H_2O_2:H_2O$ at a ratio of 1:1:48 to remove the unexposed sections of the bimetallic film. The etch rate of this solution for Bi/In bimetallic films is roughly 65 Å/sec[5], expecting the Sn/In film to have a similar etch rate the bimetallic film was developed for around 15 to 30 seconds until visually seen to be developed. Figure 12 shows microscope images of the bimetallic film after development as a thermal resist for both the air and water-immersed conditions.

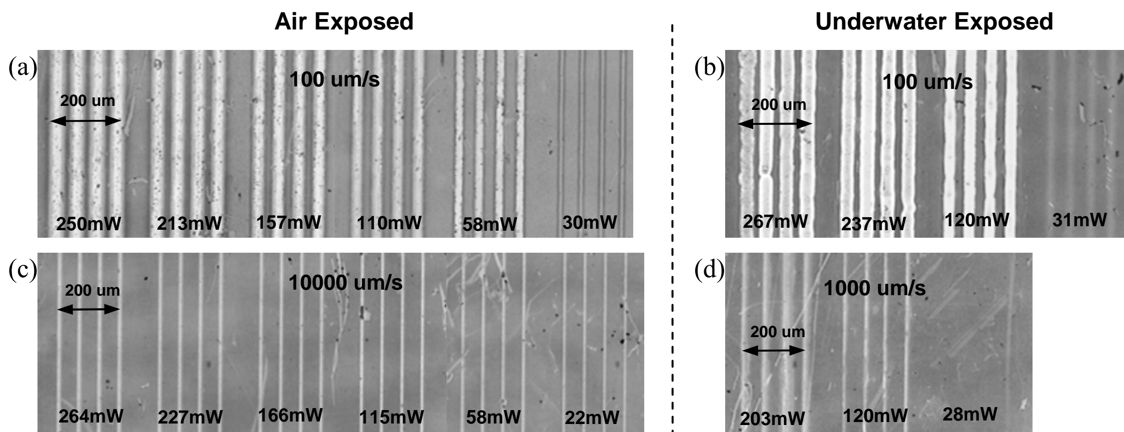

Figure 12: Microscope images for 80nm thick Sn/In bimetallic film exposed in both air and water-immersed conditions, after development as a thermal resist: (a) lines written at 100 μm/s in air, 10 μm spot, (b) written at 100 μm/s in water, 10 μm spot, (c) written at 10000 μm/s in air, 2 μm spot, and (d) written at 1000 μm/s in water, 2 μm spot.

As can be seen in Figure 12 (a) and (c), the air-written lines were successfully developed with little difficulties. For the water-immersed lines, the ones written at 100 μm/s and 1000 μm/s were able to be developed, while those written at 10000 μm/s did not. The lack of development for the faster velocity is likely due to the erosion of the oxidized material by cavitation. Further experiments will be conducted to ascertain the nature of the air/steam layer, if the air/steam bubble plays a key role in the exposure of the water-immersed films, and if its presence does affect the resulting resist exposure as seen after development.

7. TRANSPARENCY PROFILING SYSTEM FOR BIMETALLIC THIN-FILM PHOTOMASKS

In the other application of bimetallic resists, grayscale photomasks, it is important to control the exact value to which the Sn/In or Bi/In turns transparent. Grayscale mask accuracy is set by the maximum absorption to minimum absorption ratio, and the number of gray levels that can be accurately controlled. For existing commercial grayscale masks, the level of accuracy is <50 gray levels for OD changes of 1.5 to 0.4, typically. By comparison bimetallic resists have OD changes typically form >3OD to <0.22OD which should enable a much larger grayscale range. In producing bimetallic grayscale photomasks, we have found there is a non-linear relationship between the laser power and the resulting exposure for the bimetallic film. Consequently, the relationship between a bitmap's grayscale and the modulation performed by the shutter must be properly calibrated in order to produce the desired mask[6]. The calibration is dependent upon the output from the Argon laser prior to passing through the electro-optic shutter, the optical alignment and elements after the electro-optical shutter, and the properties of the bimetallic film being patterned. Previously, the calibration was performed outside of the writing process by patterning large 1 cm^2 squares using specific settings for the mask-writing system and then measuring them with an HP 8453 UV/Visible spectrometer to determine their OD/transparency. The squares need to be a minimum of 1 cm^2 since the measurement area of the spectrometer is on the same scale. This calibration method is both time consuming and limits the number of possible levels measured (e.g. a standard microscope slide fits only 6 squares). In addition, the bimetallic film's laser exposure versus transparency characteristics can vary from deposition to deposition, these complications make calibrating for a 256 level range extremely difficult using the spectrometer. An alternate and indirect method of calibrating the mask is to use it in a typical lithographic process where the resulting 3D photoresist structure can be profiled. However, this indirect method introduces several resist process variables and a multitude of factors that can influence the resulting 3D structure and make calibrating the mask just as difficult[7]. An alternative approach is to directly measure the transparency while writing. The mask's transparency is determined using measurements of the beam's intensity before and after the bimetallic layer. The distinct advantage with this method is that the calibration is done at the resolution of the pattern.

In previous experiments, the idea of using the writing laser to measure the transparency of a photomask was used to measure the change in transparency versus time for several films as they underwent oxidation[8]. In order to measure the transparency of an already patterned mask, the power level has to be sufficiently low so as not to alter the mask. However, having the laser power too low also presents problems for high OD (low transparency) samples where the laser beam can become too weak to measure after passing through the mask. Based on the same setup, the experimental system used for our latest set of experiments is shown in Figure 13 and uses similar sensors based on the OPT1010P-ND Monolithic Photodiode and Single-Supply Transimpedance Amplifier from Texas Instuments, two 24-bit Analog to Digital (A/D) converter cards based on the AD7732 from Analog Devices, and a Xilinx FPGA development board which acts as the interface between the A/D converters and the mask-writing system.

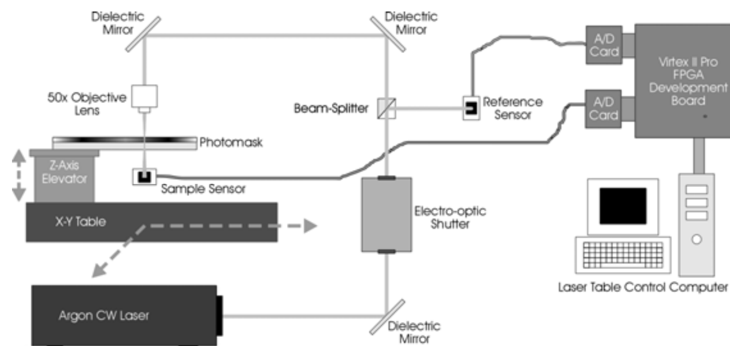

Figure 13: OD/Transparency Profiling System Setup

To perform our measurements, the photodiode sensors were adjusted to produce a near 10V output when exposed with a 1mW laser beam. The output voltage versus exposure power relationships for the photodiode sensors are shown in Figure 14. An important point to mention is that the laser beam's position and orientation on the sensor significantly influences the sensor's characteristics. This result is clearly illustrated in the difference between the reference and sample sensor characteristics where the reference sensor is exposed to the unfocussed parallel beam while the sample sensor is exposed to the laser beam after it has been focused. Both sensors are electronically identical. Another point to mention is that because the laser is primarily of a single wavelength, the transparency values that are being measured are for the exact same wavelength, which in this case is 488 nm.

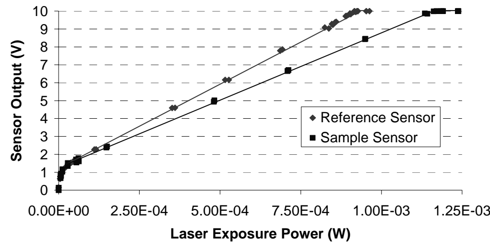

Figure 14: Photodiode Sensor Voltage vs. Power Response

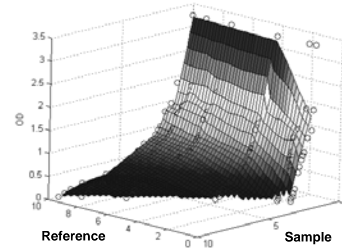

Figure 15: Sample and Reference Sensor vs. OD (488 nm)

Two methods of converting the sensor measurements into transparency values are available. One method is to determine the photomasks transparency by converting the sensor readings into laser power and then calculating the photomask's OD. This method requires calibration measurements for both the sample's OD/transparency and each sensor's power versus output voltage characteristics. Furthermore, the calculation is complicated by several factors such as the beam's position and profile when striking the sensor and the system's optics. To avoid these complications and reduce the time needed to calibrate the system, a series of known OD samples were instead measured using a range of laser powers. For each OD and laser power setting, the values for both the sample and reference sensor were recorded. The result is a 3D calibration plot, shown in Figure 15, where the photomask's transparency can be determined based on the values of both the sample and reference sensors. The calibration remains valid, so long as the optics after the beam-splitter are not altered. With the ability to profile and measure OD/transparency using the two photodiode sensors, having the photomask-writing system profile the transparency of a mask becomes possible by utilizing the X-Y table already present in the system.

8. TRANSPARENCY PROFILE MEASUREMENTS FOR BEAM-SHAPED WRITTEN PATTERNS

The high resolution of the bimetallic resists shown in Section 3 results in the written pattern being affected by the power distribution within the laser spot itself. Experiments performed previously attempted to improve the quality and uniformity of the patterns written on bimetallic films by shaping the writing laser beam[3]. The experiments involved writing mask patterns using beam-shaping techniques to modify the writing laser. Three patterns were made: first was with an unaltered Gaussian beam, second a beam shaped by a binary mask consisting of a square aperture, and lastly a beam shaped by a grayscale mask designed to provide a "top-hat" power distribution. Examples for an ideal Gaussian and "top-hat" profile are shown in Figure 16 and Figure 17, while Figure 18 illustrates the bitmap used to create the beam-shaping mask. Continuing the analysis of those experiments, the photomasks that were previously written were examined using the transparency profiling system to quantify the differences in their transparency and consistency, as shown in Figure 19.

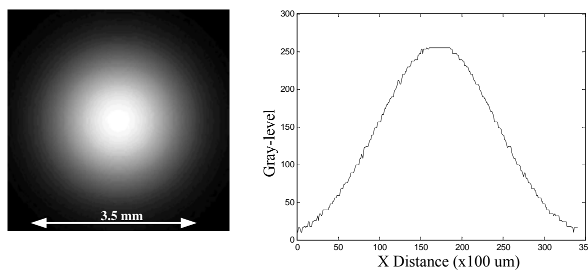

Figure 16: Ideal Gaussian and its cross-sectional profile.

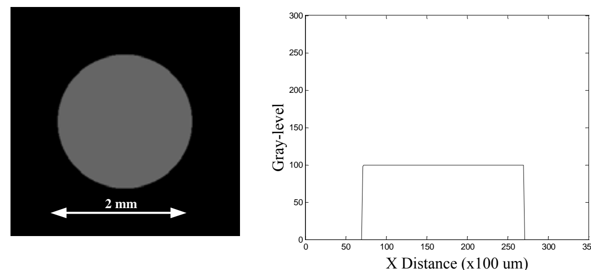

Figure 17: Ideal "top-hat" profile.

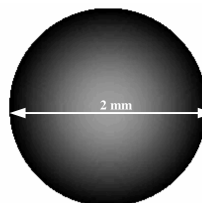

Figure 18: Bitmap image used to create the beam-shaping mask. Darker areas will result in a higher laser exposure and produce more transparent areas on the mask.

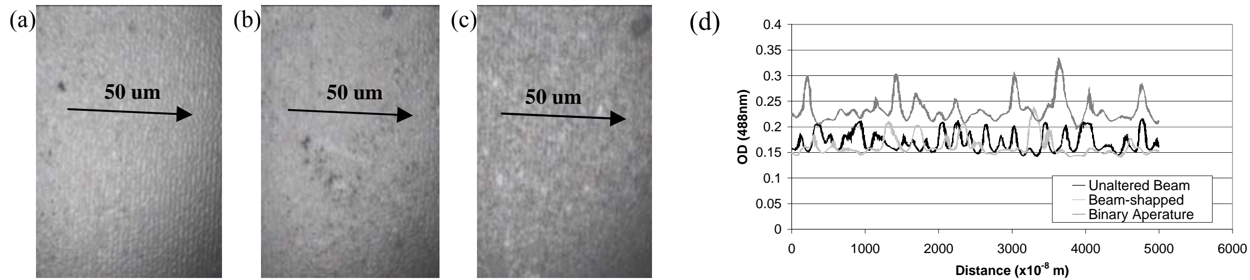

Figure 19: Transparency scans for lased squares on 40/40 nm Bi/In, using 0.1W laser power, 50× objective lens and 1 µm step size: (a) microscope images for the lased square using the unaltered beam, (b) the beam through the grayscale circular mask and (c) the beam through a binary square mask, and (d) transparency profiles for the lased squares.

From the transparency profiles and images in Figure 19, the beam-shaping mask appeared to improve the OD consistency for the film. However, a true "top-hat" laser beam should have resulted in a more improved consistency. As can be seen in Figure 19 (d), there are still significant variations with Gaussian characteristics, indicating that the writing beam was either not shaped to have an ideal "top-hat" profile or that a different shaping is required. Experiments will be conducted to verify the abilities of our beam-shaping mask and obtain a better "top-hat" profile.

9. CONCLUSION

To demonstrate a potential for exploring double exposure techniques, bimetallic resists must show both the resolutions and the ability to operate with immersion lithography. Bimetallic resists have demonstrated <42 nm structures using interference lithography at 266 nm in air. However, this result appears to be a limit of the exposure system, rather than the resist. For immersion lithography, a Sn/In film was exposed underwater and then developed showing thermal resist characteristics. The film was examined prior to and after development, finding that the exposure threshold for the water-immersed film was slightly higher than the air-written film, but not so different as to indicate a large heat loss to the water. However, exposing the films underwater was complicated by the creation of an air/steam bubble at the laser spot. It is not clear if the creation of this steam layer is needed for immersion exposures.

In the application of bimetallic resists as grayscale photomasks, we utilized two photodiode sensors with the mask-writing system to form an OD/transparency profiler. To improve the mask uniformity, a photomask was written using a beam-shaped laser and examined to determine its improvement in transparency consistency. Although indicating an improvement in the film's consistency, the transparency profiles taken still showed Gaussian characteristics and it is believed that the beam-shaping mask did not produce the desired "top-hat" power profile for the laser beam used in writing the mask. Attempts at making a better beam-shaping mask are to be performed utilizing the verification abilities now offered by the OD/transparency profiling system.

REFERENCES:

1. A.M. Biswas, J. Li, J.A. Hiserote, L.S. Melvin III, "Extension of 193 nm dry lithography to 45-nm half-pitch node: double exposure and double processing technique." *Proc. of SPIE*, Vol 6349, 63491P. 2006.
2. Y. Tu, G.H. Chapman, M.V. Sarunic, "Bimetalltic Thermall Activated films for Microfabrication, Photomasks and Data Storage." *Proc. of SPIE*, Vol 4637, 330-340. 2002.
3. J. Dykes, D. Poon, J. Wang, J. Tsui, G.H. Chapman, "Improving the Optical Characteristics of Bimetallic Grayscale Photomasks." *Proc. of SPIE*, Vol 6458, 64580T:1-12. 2007.
4. G.H. Chapman, Y. Tu, C. Choo, J. Wang, D. Poon, M. Chang, "Laser-induced Oxidation of Metallic Thin Films as a Method for Creating Grayscale Photomasks." *Proc. of SPIE*, Vol 6153, 61534G:1-12. 2006.
5. Y. Tu, G.H. Chapman, "Bi/In as Patterning and Masking Layers for Alkaline-Base Si Anisotropic Etching." *Proc. of SPIE*, Vol 4979, 87-98. 2003.
6. Y. Tu, G.H. Chapman, J. Dykes, D. Poon, C. Choo, J. Peng, "Calibrating Grayscale Direct Write Bimetallic Photomasks to Create 3D Photoresist Structures." *Proc. of SPIE*, Vol 5567, 245-256. 2004.
7. G.H. Chapman, J. Dykes, D. Poon, C. Choo, J. Wang, J. Peng, Y. Tu, "Creating Precise 3D Microstructures Using Laser Direct-write Bimetallic Thermal Resist Grayscale Photomasks." *Proc. of SPIE*, Vol 5713, 247-258. 2005.
8. D. Poon, J. Dykes, C. Choo, J. Tsui, J. Wang, G.H. Chapman, Y. Tu, P. Reynolds, A. Zanzal, "Adding Grayscale Layer to Chrome Photomasks." *Proc. of SPIE*, Vol 6349, 634931:1-12. 2006.